

EXAMINING THE MULTIFACETED PROPERTIES OF GA-DOPED BIGAXFE1-XO3 FABRICATED VIA THE MICROEMULSION TECHNIQUE

SUBHAJIT GHANA
SC19BPHDPH002

Enrollment No.
PHYSICS

Dr. SUDHAKAR SINGH
SARDAR PATEL UNIVERSITY, BALAGHAT

DECLARATION: I AS AN AUTHOR OF THIS PAPER /ARTICLE, HERE BY DECLARE THAT THE PAPER SUBMITTED BY ME FOR PUBLICATION IN THE JOURNAL IS COMPLETELY MY OWN GENUINE PAPER. IF ANY ISSUE REGARDING COPYRIGHT/PATENT/ OTHER REAL AUTHOR ARISES, THE PUBLISHER WILL NOT BE LEGALLY RESPONSIBLE. IF ANY OF SUCH MATTERS OCCUR PUBLISHER MAY REMOVE MY CONTENT FROM THE JOURNAL WEBSITE. FOR THE REASON OF CONTENT AMENDMENT /OR ANY TECHNICAL ISSUE WITH NO VISIBILITY ON WEBSITE/UPDATES, I HAVE RESUBMITTED THIS PAPER FOR THE PUBLICATION. FOR ANY PUBLICATION MATTERS OR ANY INFORMATION INTENTIONALLY HIDDEN BY ME OR OTHERWISE, I SHALL BE LEGALLY RESPONSIBLE. (COMPLETE DECLARATION OF THE AUTHOR AT THE LAST PAGE OF THIS PAPER /ARTICLE.

Abstract

The impact of Ga-replacement on bismuth ferrite $BiGaxFe_{1-x}O_3$ ($x = 0, 0.05, 0.10, 0.15, 0.20,$ and 0.25) properties was investigated, which was fabricated utilizing a microemulsion course. X-beam diffraction examination affirmed that examples had a solitary stage rhombohedral design with space bunch $R\bar{3}c$. The grouping of Ga affected different properties like underlying boundaries, translucent size, porosity, and unit cell volume. The examples showed prominent qualities for the dielectric consistent, digression misfortune, and dielectric misfortune in the low-recurrence range, which declined as the recurrence expanded because of various polarizations. The review takes a gander at the combined materials' underlying, electrical, and ferroelectric attributes at various doping levels and organizations. The review explains the effects of Ga doping on the material's properties utilizing strategies including ferroelectric tests, FTIR spectroscopy, flow voltage examination, and X-beam diffraction. As the doping level builds, the outcomes show extensive changes in the crystallite size, thickness, polarization qualities, and grid boundaries. All the more explicitly, the information demonstrate that with expanding doping levels, there is a reduction in cell volume, an expansion in porosity, and changes in electrical conductivity and ferroelectric conduct. These revelations advance our insight into perovskite oxide materials and the forthcoming purposes of ferroelectric and strong state gadgets.

Keywords: Ga-Doped, Bigaxfe1-Xo3, Fabricated, Microemulsion, Technique

1. INTRODUCTION

The quest for novel materials with tweaked highlights has drawn a ton of interest as of late from a great many logical fields. Of these, perovskite oxides have shown extraordinary commitment in light of their versatile qualities and broad purposes in detecting, hardware, catalysis, and energy stockpiling. The multiferroic character of bismuth ferrite (BiFeO_3), which consolidates antiferromagnetic and ferroelectric properties at ordinary temperature, has drawn in a ton of consideration among researchers. In any case, to completely understand BiFeO_3 's true capacity and extend its utilization into different fields, researchers have searched for ways of improving and change its attributes. Doping with various components to change a substance's primary, electrical, attractive, optical, and synergist properties is one strategy for doing as such. Doping with gallium (Ga) specifically has shown guarantee since it can make outstanding changes the qualities of perovskite oxides. In this paper, we orchestrate and portray Ga-doped BiFeO_3 , otherwise called $\text{BiGa}_x\text{Fe}_{1-x}\text{O}_3$, which is made by the microemulsion strategy. This interaction makes it conceivable to unequivocally direct the morphology, content, and crystallinity of the orchestrated materials, considering the customization of their attributes for specific purposes. Gallium presents energizing choices for changing the electrical construction, attractive way of behaving, and optical highlights of the BiFeO_3 grid. Ga doping opens up opportunities for new gadget abilities and applications by changing the band gap, the attractive requesting in the material, and the conveyance of charge transporters. Besides, the microemulsion strategy offers an adaptable stage for the combination of intricate oxide materials with modified nanostructures and syntheses. Exact command over the size, shape, and crystallinity of the nanoparticles can be acquired by changing the boundaries of the microemulsion framework, including surfactant content, oil-to-water proportion, and response conditions. In this regard, the objective of this work is to completely look at the many credits of Ga-doped BiFeO_3 that was delivered by means of the microemulsion strategy. We will investigate the manufactured materials' optical, dielectric, attractive, photocatalytic, and antibacterial properties to give understanding into their potential purposes in various businesses, including biomedical designing, ecological remediation, optoelectronics, and catalysis.

2. REVIEW OF LITREATURE

Jagadeeshwaran (2020) The effect of cobalt substitution in the nickel aluminate phone structure has been the essential point of convergence of our continuous work. The material precipitation technique was used to make the aluminate tests. The optical and essential properties of the NiAl_2O_4 , CoAl_2O_4 , and $\text{Ni}_{0.5}\text{Co}_{0.5}\text{Al}_2\text{O}_4$ materials were examined by UV DRS absorbance range investigation and X-bar diffraction. Through investigation of its diffraction best, the XRD configuration checks the cubic stage with the room gathering of $Fd\ 3\ m$. The improvement of

NiAl₂O₄, CoAl₂O₄, and Ni_{0.5}Co_{0.5}Al₂O₄ process is loosened up by the UV osmosis tops at 360, 480, 551, 580, and 621 nm.

Wu (2020) Due to its tiny size, locale result, quantum tunneling influence, and possible applications in customary materials, clinical gadgets, contraptions, various regions, and coatings, nanomaterials — another material — certainly stick out. This article truly presents the effects of grain size, creation technique, and breaking point structures on the real credits of nanomaterials as well as the assurance of nanoparticles. The current status of sensible movement and the extent of purposes for nanomaterials are discussed. Nanomaterials are dominating than common materials because of their intriguing properties.

Suresh et al. (2019) The continuous concentrate successfully made pure and change metal titanium (Ti)- doped LaFe_{1-x}Ti_xO₃ nanoparticles in various molar degrees of 0.2, 0.4, and 0.6 using the fluid amalgamation system. The fitted models were cleaned and warmed to 600 °C for four hours in a radiator. Ti doped LaFeO₃ and LaFeO₃ show stage orthorhombic improvement, which is avowed by X-shaft diffraction. assessment. Through coherent investigation using energy dispersive X-radiates ., the stoichiometric assessment was performed. Area release sifting electron microscopy (FESEM) has been used to focus on the smaller than expected hidden components of district morphology. Additionally, significant standard transmission electron microscopy. assessment was used to also investigate the district nanocrystalline of the titanium (Ti)- doped LaFe_{1-x}Ti_xO₃.

Dontsova (2019) The attributes, combination, and utilizations of nanocomposite metal oxide materials, especially TiO₂, ZnO, SnO₂, ZrO₂, and Fe₃O₄, for environmental objects are believed to be canvassed in this article. It has been found that nanomaterials dependent on them have extraordinary commitment for use in the environmental pathway, particularly as photocatalysts, sorbents, and extremely touchy gasoline sensors. These metallic oxides have surface peculiarities, crystallochemical properties, and surface designs that seem when they come into contact with water or air. It has been shown that these components are critical in obtaining the sorption and synergist properties of the nanomaterials.

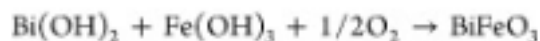
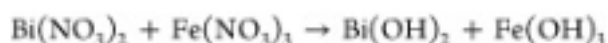
3. MATERIALS AND METHODS

3.1 Chemicals and Reagents

The precured metal salts, specifically Bi(NO₃)₂·6H₂O, Ga(NO₃)₃, and Fe(NO₃)₃·6H₂O, were acquired from Sigma-Aldrich, though Merck gave NH₄OH, CTAB, and gem violet (CV) color. All through the entire investigation, refined water was utilized to plan stock arrangements and weakenings.

3.2 Synthesis of BFO and BiGaxFe1-xO3 NPs

A technique was followed to create unadulterated BiFeO₃ and BiGaxFe1-xO₃ NPs (where x = 0.00, 0.05, 0.10, 0.15, 0.20, and 0.25). To make the important arrangements, the metal nitrates (stoichiometric proportion) were broken down in water. Arrangements were joined in a 500 mL measuring utensil and warmed for roughly 30 minutes at 60 °C. At the point when the temperature arrived at the ideal level, the intensity was switched off, however blending was continued onward. With the utilization of an ammonium hydroxide arrangement, the pH was brought to 11. Then, the blend was unsettled for seven hours utilizing an attractive hot plate stirrer. Until the pH of the arrangement arrived at nonpartisan, it was over and again flushed. From that point onward, the encourages were over and over cleaned with deionized water and dried at 150 °C for 12 hours. The materials that had been broiler dried were finely powdered and afterward calcined at 950 °C for six hours. The proposed responses for the amalgamation of BFO development are portrayed by equations 1 and 2.



3.3 Characterization

The nanomaterials made by the microemulsion technique were inspected using different deliberate techniques. X-beam diffraction (Philips X-beam Spunky Ace 3040/60) was utilized to investigate crystallinity, and P-E circle following was utilized to survey ferroelectric qualities utilizing the M-S Brilliant instrument (USA). With the utilization of Raman spectroscopy and FTIR (Nexus-470 spectrophotometer), the synthetic connection between the components was affirmed. A Wayneker WK6500B LCR meter was utilized to quantify the dielectric qualities in the recurrence scope of 20 Hz to 0.2 GHz, while a Keithley 2400 m was utilized to record the I-V (flow voltage) estimation. At last, a Convey 60 spectrophotometer was utilized for the UV-vis investigations.

3.4 Photocatalytic Activity

Under visible light, the photocatalytic possibilities of BiFeO₃ and BiGaxFe1-xO₃ were assessed for CV color. All through the photocatalytic explore, 150 mL of a CV color arrangement was joined with 15 mg of the photocatalyst. Following 20 minutes of twirling in obscurity, the combination was presented to a 160 W Xe light. Utilizing a Convey 60 spectrophotometer, the important

number of tests were taken from the color arrangement at coordinated stretches, and the absorbance at 588 nm was recorded. The impetus powder was disposed of from the arrangement by centrifuging it before every absorbance estimation. The absorbance readings were utilized to ascertain the CV focus, and Condition 3 was utilized to assess the rate crumbling. Here, A_0 and A_t represent the absorbance values at time "0" and time "t," respectively.

$$\text{Degradation}(\%) = 1 - \frac{A_t}{A_0}$$

4. RESULTS AND DISCUSSION

4.1 XRD Analysis

Table 1 sums up the cross-section qualities, normal grain sizes, and gem design of the nanocrystalline BFOG. Each XRD top relates suitably with the norm (JCPDS document number 71-2494), exhibiting the production of the perovskite structure.

Table 1: Effect of Ga Doping on Various $\text{BiGa}_x\text{Fe}_{1-x}\text{O}_3$ NP Structural Parameters

Doping Content (x, y)	Cell Volume (\AA^3)	Lattice Constant a (\AA)	Lattice Constant c (\AA)	c/a Ratio	Crystallite Size (nm)	X-ray Density (g cm^{-3})	Bulk Density (g cm^{-3})	Porosity (%)	Dislocation Density	Strain
0.01	412.9	6.15	14.12	3.15	35.4	3.82	2.36	51	1.20	0.512
0.06	370.2	6.71	14.47	3.18	33.7	3.55	2.39	50	2.15	0.482
0.11	370.3	6.85	14.52	3.20	32.05	3.65	2.41	55	2.09	0.512
0.17	342.8	6.14	14.71	3.25	31.4	3.81	2.25	53	2.05	0.536
0.22	388.7	6.18	14.62	3.26	30.8	3.80	2.32	55	0.81	0.512
0.26	371.2	6.71	14.71	3.30	32.5	3.78	2.15	60	0.89	0.492

The information presented illustrates the differences in characteristics between Ga-doped $\text{BiGa}_x\text{Fe}_{1-x}\text{O}_3$ materials created by the microemulsion technique at different doping concentrations. Some significant changes are observed in several basic parameters as the doping focus (x, y) grows from 0.01 to 0.26. First, while the doping level increases, the cell volume drops

from 412.9 \AA^3 to 371.2 \AA^3 , showing a decrease in the volume involved by the unit cell. The grid constants a and c also fall with this decrease, which results in a minor increase in the c/a proportion and suggests a more minimized crystal structure with higher doping levels. Moreover, while the doping level rises, the crystallite size steadily lowers from 35.4 nm to 30.8 nm, showing a refinement in the material's grain size. By decreasing grain limit effects, this decrease in crystallite size might work on the mechanical and electrical properties of the material.

The material's X-ray density fluctuates slightly yet by and large tends to drop, suggesting that increased doping levels cause the material's density to decrease. Similar to this, with more prominent doping concentrations, the porosity rises from 51% to 60% and the mass density falls from 2.36 g cm^{-3} to 2.15 g cm^{-3} , showing a more porous structure. It's interesting to take note of that the dislocation density varies with doping fixation, cresting at 0.06 and afterward declining at more elevated levels. This implies that the centralization of doping and the existence of flaws in the material communicate complicatedly and may affect the material's mechanical and electrical properties. Lastly, the material's strain varies however mostly stays inside a small reach, suggesting that the grid is slightly stressed by compressive or tensile forces. This stress might be caused by gallium ions being integrated into the crystal grid. In general, the data gave sheds light on the structural and physical characteristics of Ga-doped $\text{BiGa}_x\text{Fe}_{1-x}\text{O}_3$ materials, emphasizing how significant factors including cell volume, crystallite size, density, porosity, and imperfection density are impacted by doping fixation. These results advance our insight into the improvement of perovskite oxide materials' microstructural development and execution enhancement for a scope of mechanical applications.

4.2 FTIR Spectroscopic Analysis

The unadulterated and Ga-substituted BiFeO_3 NPs have been portrayed using the FTIR spectra somewhere in the range of 400 and 4000 cm^{-1} . The octahedral type of the FeO_6 unit exhibits twisting/bended vibrations of the O-Fe-O security, shown by an absorption edge meant as $E(\text{T}08)$ at $440\text{-}450 \text{ cm}^{-1}$. Two groups of $E(\text{T}09)$ and $A_1(\text{T}04)$ modes were recognized for the scope of 480 to 680 cm^{-1} . The absorption band mode in FeO_6 is around 575 cm^{-1} , yet the vibrational method of the Bi/Ga-O bond is close to 550 cm^{-1} , because of the elongated vibrations of the Fe-O bond. The FTIR spectra of the various samples also show the shifting of their dynamic infrared modes (signified by the red bolt). It is clear which shows an assortment of FT-IR spectra covering the wavenumber scope of $300\text{-}4000 \text{ cm}^{-1}$, that the spectra's locations have changed. By increasing the centralization of Ga, the absorption top shifts slightly toward a lower wavenumber; this shift might be caused by Ga's smaller ionic radius than Fe's. Besides, this shift suggests that octahedron deformity with the Ga-substitution has twisted the Bi-O and Fe-O bonds.³⁶ Because of the

antisymmetric stretching of hydroxyl ions and H₂O ions, respectively, each sample exhibits a wide absorption band in the 3300-3600 cm⁻¹ territory.

4.3 Current Voltage (I–V) Analysis

Two test I-V measurements were performed using pristine and doped BiGaxFe_{1-x}O₃ in the 20–20 V reach to ascertain the effects of Ga doping on the electrical conductivity of the doped material. Pellets were synthesized with a constant measurement of 820 mm and a width of 2.16–2.31 mm. The recipe presented in condition 4 was used to register the surface region of the pellets.

$$\sigma = \frac{W}{RA}$$

The doped sample's (I-V) response is direct, however unadulterated BiFeO₃'s (I-V) exhibits an inverse S shape, suggesting semiconductive movement. As the dopant fixation was raised, the doped sample's current-voltage relationship stayed almost direct. This peculiarity was demonstrated to be caused by Ga doping and is suggestive of higher EC contrasted with BiFeO₃. Specifically, the octahedral locations of the Ga³⁺ and Fe³⁺ ions in the perovskite materials are switched. The EC (I-V) conduct of Ga was empowering when contrasted with the Fe ions in the BiFeO₃ sample.

4.4 Electrical Polarization

Pellets measuring 7 mm in width and covered with silver paste were used as the electrodes in ferroelectric research of BiGaxFe_{1-x}O₃. The incited extremity was identified using a PUND (positive up and negative down) mode, which simplified it to subtract non-ferroelectric elements like space charge and spillage flow. Flow spillage is a significant issue that complicates the measurement of the hysteresis circle for perovskite ferroelectrics working at high temperatures. The room-temperature measurements of the BiGaxFe_{1-x}O₃ polarization field hysteresis loops and the pristine BFO. Each polarization circle has a sunken structure and demonstrates intrinsic ferroelectric characteristics. Doping substituents into the perovskite structure changed the P-E loops in every mixture. The curves slowly start to straighten at both the positive and negative field regions, exhibit a rise in polarization in the electric field's positive locale, and a fall in polarization in its negative district. This occasion could be the consequence of their characteristic being changed to lossy trends by an escape or destabilization at the negative post area. The pristine sample displays a lossy response, and it has been seen in the doped samples that this response diminishes with increasing Ga³⁺ fixation, suggesting that the collection of extra charge carriers at the connection point is responsible for the material's increased resistivity.⁴² Since the mass

material's ferroelectricity is transcendently caused by the stereo chemically dynamic Bi-6s solitary pair, the impact of supplanting Fe with Ga on polarization is fairly small; as a result, polarization is somewhat decreased after doping. The determined values of saturation polarization (Ps), Ps/Pr, and remanence polarization (Pr) for every focus are shown in Table 2.

Table 2: Variation in BiGaxFe1-xO3 (x, y = 0.0–0.25) NPs' Ferroelectric Parameters as the Dopant Content Increases

Doping Content	Composition	Pr ($\mu\text{C}\cdot\text{cm}^2 \times 10^{-4}$)	Ec (kV/cm)	Ps ($\mu\text{C}\cdot\text{cm}^2 \times 10^{-4}$)
0.1	BFO	7.12	3.25	6.12
0.06	BFOG1	5.25	3.21	5.25
0.06	BFOG1	5.32	3.21	5.23
0.18	BFOG3	4.12	2.25	3.12
0.22	BFOG4	4.25	2.25	3.26
0.30	BFOG5	3.25	3.12	2.21

The information supplied illustrates the differences in saturation polarization (Ps), remainder polarization (Pr), and coercive field (Ec) for Ga-doped BiGaxFe1-xO3 materials at various doping concentrations and compositions. We see trends in the materials' polarization properties as the doping level rises. The leftover polarization (Pr) is measured at $7.12 \mu\text{C}\cdot\text{cm}^2 \times 10^{-4}$, with a coercive field (Ec) of 3.25 kV/cm and a saturation polarization (Ps) of $6.12 \mu\text{C}\cdot\text{cm}^2 \times 10^{-4}$, starting with the pristine BiFeO3 (BFO) composition at 0.1 doping content. Ferroelectric materials are portrayed by a modest coercive field and generally high polarization, as shown by these numbers. We find that the system exhibits various degrees of polarization characteristics when gallium (Ga) dopants, represented by compositions BFOG1, BFOG3, BFOG4, and BFOG5, are added at doping concentrations of 0.06, 0.18, 0.22, and 0.30, respectively. For example, two information points are supplied at a 0.06 doping happy with composition BFOG1, suggesting the possibility of experimental replication or measurement. While Ec stays the same, the two locations exhibit somewhat lower Pr and Ps when contrasted with unadulterated BFO.

There is an overall propensity of decreased polarization values all through the various compositions as the doping content rises further. For instance, with composition BFOG5, at 0.30 doping focus, Pr declines to $3.25 \mu\text{C}\cdot\text{cm}^2 \times 10^{-4}$, Ec rises to 3.12 kV/cm, and Ps drops to $2.21 \mu\text{C}\cdot\text{cm}^2 \times 10^{-4}$. The decrease in polarization features can be explained by the suppression of ferroelectric domains and space wall movement resulting from the disturbance of ferroelectric request achieved by the insertion of Ga ions into the BiFeO3 cross section. Generally speaking, the information highlights how composition and doping level influence the ferroelectric

characteristics of Ga-doped $\text{BiGaxFe}_{1-x}\text{O}_3$ materials, offering data about their uses in solid-state electronics and ferroelectric devices.

5.CONCLUSION

The work concludes with an exhaustive examination of the synthesis, characteristics, and attributes of Ga-doped $\text{BiGaxFe}_{1-x}\text{O}_3$ nanoparticles made using the microemulsion strategy. We have explained the structural, electrical, and ferroelectric properties of the created materials at various compositions and doping concentrations by a series of deliberate tests and analysis. As the doping content rose, the X-ray diffraction examination showed changes in the grid parameters, crystallite size, and density, showing the materials' structural advancement. Ga doping-prompted octahedral distortions and compound interactions were shown by FTIR spectroscopy. The semiconductor characteristic of the doped materials was demonstrated through electrical portrayal using flow voltage analysis, where Ga doping resulted in increased electrical conductivity. Ferroelectric experiments also showed patterns in polarization properties: as doping level rose, there was a general decrease in residual and saturation polarization. These results highlight the perplexing interactions that exist between the composition, doping fixation, and material characteristics of Ga-doped $\text{BiGaxFe}_{1-x}\text{O}_3$ nanoparticles. In light of everything, this work advances our insight into perovskite oxide materials and establishes the preparation for future uses of them in various industries, including ferroelectric devices, solid-state electronics, and catalysis.

REFERENCES

1. C. Jagadeeshwaran (2020)" Structural, Optical, Magnetic, and Electrical Properties of $\text{Ni}_{0.5}\text{Co}_{0.5}\text{Al}_2\text{O}_4$ System" *Journal of Superconductivity and Novel Magnetism* (2020) 33:1765–1772
2. Sasikala, C., Suresh, G., Durairaj, N. et al. (2019) Chemical, Morphological, Structural, Optical, and Magnetic Properties of Transition Metal Titanium (Ti)- Doped LaFeO_3 Nanoparticles. *J Supercond Nov Magn* 32, 1791–1797.
3. Tetiana A. Dontsova, Svitlana V. Nahirniak, Ihor M. Astrelin, (2019) "Metaloxide Nanomaterials and Nanocomposites of Ecological Purpose", *Journal of Nanomaterials*, vol. 2019, Article ID 5942194, 31 pages.
4. Toksha, BG, Sagar E. Shirsath, Patange, SM & Jadhav, KM 2008, 'Structural investigations and magnetic properties of cobalt ferrite nanoparticles prepared by sol-gel auto combustion method', *Solid State Communications*, vol. 147, no. 11-12, pp. 479-483.
5. Vaidyanathan, G & Sendhilnathan, S 2008, 'Synthesis and magnetic properties of Co-Zn magnetic fluid', *Journal of Magnetism and Magnetic Materials*, vol. 320, no. 6, pp. 803- 805.

6. Vaidyanathan, G, Sendhilnathan, S & Arulmurugan, R 2007, 'Structural and magnetic properties of $\text{Co}_{1-x}\text{Zn}_x\text{Fe}_2\text{O}_4$ nanoparticles by co-precipitation method', *Journal of Magnetism and Magnetic Materials*, vol. 313, no. 2, pp. 293- 299
7. Veena Gopalan, E, Al-Omari, IA, Malini, KA, Joy, PA, Sakthi Kumar, D, Yasuhiko Yoshida & Anantharaman, MR 2009, 'Impact of zinc substitution on the structural and magnetic properties of chemically derived nanosized manganese zinc mixed ferrites', *Journal of Magnetism and Magnetic Materials*, vol. 321, no. 8, pp. 1092-1099.
8. Venkataraju, C, Sathishkumar, G & Sivakumar, K 2010, 'Effect of cation distribution on the structural and magnetic properties of nickel substituted nanosized Mn-Zn ferrites prepared by co-precipitation method', *Journal of Magnetism and Magnetic Materials*, vol. 322, no. 2, pp. 230-233.
9. Venkataraju, C, Sathishkumar, G & Sivakumar, K 2010, 'Effect of cation distribution on the structural and magnetic properties of nickel substituted nanosized Mn-Zn ferrites prepared by co-precipitation method', *Journal of Magnetism and Magnetic Materials*, vol. 322, no. 2, pp. 230-233.
10. Virden, A, Wells, S & O'Grady, K 2007, 'Physical and magnetic properties of highly anisotropic cobalt ferrite particles', *Journal of Magnetism and Magnetic Materials*, vol. 316, pp. e768-e771.
11. Vuk Uskokovic, Miha Drogenik & Irena Ban 2004, 'The characterization of nanosized nickel-zinc ferrites synthesized within reverse micelles of CTAB/1-hexanol/water microemulsion', *Journal of Magnetism and Magnetic Materials*, vol. 284, pp. 294-302.
12. Wei-Chih Hsu, Chen, SC, Kuo, PC, Lie, CT & Tsai, WS 2004, 'Preparation of NiCuZn ferrite nanoparticles from chemical co-precipitation method and the magnetic properties after sintering', *Materials Science and Engineering B*, vol. 111, no. 2- 3, pp. 142-149.
13. Wongsaprom, K & Maensiri, S 2013, 'Synthesis and Room Temperature Magnetic Behaviour of Nickel Oxide Nanocrystallites', *Chiang Mai Journal of Science*, vol. 40, no. 1, pp. 99-108.
14. Wu, Qiong, Miao, Wei-shou, Zhang, Yi-du, Gao, Han-jun and Hui, David. "Mechanical properties of nanomaterials: A review" *Nanotechnology Reviews*, vol. 9, no. 1, 2020, pp. 259-273
15. Xue Cao, Guang Liu, Yiming Wang, Jianhua Li & Ruoyu Hong 2010, 'Preparation of octahedral shaped $\text{Mn}_{0.8}\text{Zn}_{0.2}\text{Fe}_2\text{O}_4$ ferrites via co-precipitation', *Journal of Alloys and Compounds*, vol. 497, no. 1-2, pp. L9-L12.

Author's Declaration

I as an author of the above research paper/article, hereby, declare that the content of this paper is prepared by me and if any person having copyright issue or patent or anything otherwise related to the content, I shall always be legally responsible for any issue. For the reason of invisibility of my research paper on the website/amendments/updates, I have resubmitted my paper for publication on the same date. If any data or information given by me is not correct, I shall always be legally responsible. With my whole responsibility legally and formally have intimated the publisher (Publisher) that my paper has been checked by my guide (if any) or expert to make it sure that paper is technically right and there in no unaccepted plagiarism and hentriacontane is genuinely mine. If any issue arises related to Plagiarism/ Guide Name/ Educational Qualification/ Designation/ Address of my university/college/institution/ Structure or Formatting/ Resubmission /Submission /Copyright /Patent/Submission for any higher degree or Job/Primary Data/Secondary Data Issues. I will be solely/entirely responsible for any legal issues. I have been informed that the most of the data from the website is invisible or shuffled or vanished from the database due to some technical fault or hacking and therefore the process of resubmission is there for the scholars/students who finds trouble in getting their paper on the website. At the time of resubmission of my paper I take all the legal and formal responsibilities, If I hide or do not submit the copy of my original documents (Andhra/Driving License/Any Identity Proof and Photo) in spite of demand from the publisher then my paper maybe rejected or removed from the website anytime and may not be consider for verification. I accept the fact that as the content of this paper and the resubmission legal responsibilities and reasons are only mine then the Publisher (Airo International Journal/Airo National Research Journal) is never responsible. I also declare that if publisher finds Any complication or error or anything hidden or implemented otherwise, my paper maybe removed from the website or the watermark of remark/actuality maybe mentioned on my paper. Even if anything is found illegal publisher may also take legal action against me

SUBHAJIT GHANA
Dr. SUDHAKAR SINGH
